Journal of Neuropathology and Experimental Neurology

Vol. 58, No. 9
September, 1999
pp. 1010–1019

Distribution of Active Glycogen Synthase Kinase 3β (GSK-3β) in Brains Staged for Alzheimer Disease Neurofibrillary Changes

JIN-JING PEI, MD, PHD, EVA BRAAK, PHD, HEIKO BRAAK, MD, PHD, INGE GRUNDKE-IQBAL, PHD, KHALID IQBAL, PHD, BENGT WINBLAD, MD, PHD, AND RICHARD F. COWBURN, PHD

Abstract. Accumulation of paired helical filaments (PHFs) in neurofibrillary tangles, neuropil threads, and dystrophic neurites is one of the major neuropathological hallmarks of Alzheimer disease (AD). The principal protein subunit of PHFs is the abnormally hyperphosphorylated tau. Glycogen synthase kinase 3β (GSK-3β) is one of the candidate kinases involved in PHF-tau formation. To play a role in PHF-tau formation, it would be expected that GSK-3β is active in tangle bearing neurons. In the present study, we investigated the regional and intracellular distributions of active and inactive forms of GSK-3β in brains staged for neurofibrillary changes. We found that neurons with tangle-like inclusions positive for active, but not inactive, GSK-3β appear initially in the Pre-α layer of the entorhinal cortex and extend to other brain regions, coincident with the sequence of the development of neurofibrillary changes. Active, but not inactive, GSK-3β was found to initially accumulate in the cytoplasm of pretangle neurons. These data provide direct in situ evidence that is consistent with the involvement of GSK-3β in PHF-tau formation.

Key Words: Alzheimer disease; Glycogen synthase kinase 3β; Neurofibrillary changes.

INTRODUCTION

Intracellular deposition of paired helical filaments (PHFs) in neurofibrillary tangles (NFTs), dystrophic neurites, and neuropil threads (NTs) is one of the major neuropathological features of Alzheimer disease (AD) (2). The principal protein subunit of PHF is abnormally hyperphosphorylated tau (3–6). Neurofibrillary changes are thought to result in the symptoms of dementia in AD patients (7–13). However, the mechanisms leading to PHF formation are not clear. It has been suggested that abnormal hyperphosphorylation of tau in AD is due to an imbalance in tau protein kinases/phosphatases. Although a number of candidates including glycogen synthase kinase 3 (GSK-3) (14, 15), mitogen-activated protein kinase (MAPK) (16, 17), and cyclin-dependent kinase 5 (cdk5) (18, 19) have been proposed, the kinases responsible for the formation of abnormally hyperphosphorylated tau in AD brain remain elusive.

GSK-3 was originally identified as a protein kinase that phosphorylated and inactivated glycogen synthase (20). Unlike other extracellular signal-regulated protein kinases, GSK-3 is fully active in unstimulated cells and is inhibited in response to insulin/insulin-like growth factor-1 (IGF-1), growth factors and other signals (21). Down-regulation of GSK-3 activity is believed to involve phosphorylation of an N-terminal serine-21 residue for GSK-3α and serine-9 for GSK-3β (22–24). Up-regulation of GSK-3β activity appears to occur through its phosphorylation at tyrosine-216 and dephosphorylation at serine-9 (25–27). The mechanisms involved in maintaining the activity of GSK-3 in AD brain remains unknown.

Both GSK-3α and GSK-3β can modify in vitro normal tau to a highly phosphorylated form that bears PHF epitopes and which exhibits a migration pattern on electrophoretic gels similar to PHF (14, 15, 18, 28–30). GSK-3α phosphorylates serine-235 and serine-404, whereas GSK-3β phosphorylates serine-199/202, threonine-231, serine-396/404, and serine-413 (14, 15, 28, 31–35). In addition, GSK-3α and GSK-3β have been found to both induce PHF-like tau phosphorylation in intact cells (36–39), leading to a reduced microtubule assembly (38, 39). Inhibition of GSK-3 activity by insulin, IGF-1, or lithium reduces tau phosphorylation and promotes tau binding to microtubules in cultured human neurons (40, 41). Such studies suggest that the GSK-3 activity is likely to contribute to the formation of abnormally hyperphosphorylated tau in AD brain.

Both GSK-3α and GSK-3β (α/β = 1.5/1), as well as tau, are enriched in brain (31, 42, 43) and found to be associated with the cytoskeleton (15, 32). Although GSK-3β has been preferentially found in NFT affected neurons (44, 45), the presence of active GSK-3β has not been characterized in pretangle neurons. Since the formation of abnormally hyperphosphorylated tau is known to start in Pre-α neurons of the entorhinal cortex and then extend to other brain regions in a predictable sequence (1), we investigated in the present study the distribution of both active and inactive forms of GSK-3β, as well as abnormally hyperphosphorylated tau in entorhinal cortex, hippocampal formation, and temporal cortical regions of human brains staged for the progression of neurofibrillary changes (1). We found the active GSK-3β and the abnormally hyperphosphorylated tau had similar topographic

From the Karolinska Institute, NEUROTEC, Section for Geriatric Medicine (J-JP, BW, RFC), Novum, KFC, S-141 86, Huddinge, Sweden; Department of Anatomy (EB, HB), J.W. Goethe University, Theodor Stern Kai 7, Frankfurt, Germany; New York Institute for Basic Research in Developmental Disabilities (IG-I, KI), Staten Island, New York.

Correspondence to: Jin-Jing Pei, Karolinska Institute, NEUROTEC, Section for Geriatric Medicine, Novum, KFC, S-141 86, Huddinge, Sweden.

distribution from very early to late stages of AD neurofibrillary pathology.

MATERIALS AND METHODS

Antibodies

Affinity-purified rabbit polyclonal phosphospecific antibodies *GSK-3β Tyrosine-216* (active form) and *GSK-3β Serine-9* (inactive form) were bought from QCB™ (Hopkinton, MA). Mouse monoclonal phosphate dependent antibody (mAb) AT8, which recognizes serine-202 and Threonine-205 of PHF-tau, was purchased from Innogenetics (anti-human PHF-tau, Zwujndrecht, Belgium).

Materials

Brains from 35 cases, aged 23–92 years were obtained at routine autopsy (Table). Blocks of temporal lobe including entorhinal, hippocampal, and temporal cortices, and/or amygdala were fixed by immersion in a mixture of 4% paraformaldehyde and picric acid, pH 7.0. Ten tissue blocks were subsequently embedded in paraffin and 8 tissue blocks in polyethylene glycol (PEG). Tissues embedded in paraffin were sectioned at 12 μm. Frozen tissues and tissues embedded in PEG were sectioned at 50–100 μm.

Brain Staging

Aldehyde fuchsin-Darrow red staining was used for topographic orientation (46). Two sections were visualized by the Gallyas silver-iodide technique for demonstration of neurofibrillary changes (47) and by immunocytochemistry with mAb AT8 for demonstration of PHF-tau pathology (48). Demonstration of amyloid deposits was made by selective silver staining (49).

All cases were classified by applying the histopathological staging system for neurofibrillary changes and amyloid deposition as described previously (1, 12). This staging procedure permits the differentiation of 6 stages (Table) with increasing severity of neurofibrillary changes, mainly in the entorhinal cortex/hippocampal formation. The transentorhinal stage I was defined by the selective involvement of NFTs and numerous dendritic NTs in projecting cells residing within the transentorhinal region. Accentuated transentorhinal pathology and a very mild involvement of the entorhinal Pre-α and first Ammon's horn sector is seen in the transentorhinal stage II. The limbic stages, III/IV, showed severe changes in the entorhinal region and hippocampal formation in addition to the transentorhinal region, with changes spreading within the limbic system. The isocortical stages, V/VI, were characterized by severe widespread destruction of limbic regions and in addition involvement of the isocortical association areas.

Tissues were classified also with respect to the extent of amyloid deposition (1). In this classification, the term amyloid refers to plaque-like deposits with or without a neuritic component. Stage 0 was characterized by the total absence of amyloid deposits. Stage A showed a few plaques in the basal isocortex. Stage B showed many plaques in the basal isocortex and allocortex. Stage C showed large numbers of plaques in all parts of the cortex.

TABLE
Sex, Age, and Neuropathological Staging of Accumulation of Both Amyloid Deposits (A–C) and Neurofibrillary (NF) Changes (I–VI)

Case	Sex	Age	Amyloid deposits	NF changes
1099/96	M	38	0	0
1230/96	F	45	0	0
1097/96	M	26	0	0
1086/96	F	28	0	0
[b]970/96	F	38	0	0
[b]1030/96	M	23	0	0
1117/96	F	70	0	I
26/97	F	66	0	II
1163/96	M	57	0	II
1117/96	F	70	0	II
1118/96	F	66	0	II
[a]87/90	M	30	0	II
[a]86/91	M	87	0	II
[a]66/90	F	80	0	II
1069/96	F	72	0	III
187/97	F	86	0	III
596/97	F	86	0	III
376/97	M	?	0	III
[a]499/91	F	87	0	III
[a]188/89	F	92	0	III
[a]180/91	M	80	B	III
[a]9/91	F	82	B	III
[a]83/91	F	86	C	III
890706	F	79	A	IV
[a]146/89	M	55	C	IV
[a]150/89	M	88	C	IV
122/70	M	65	B	V
[b]55/53	F	77	B	V
[b]6/94	F	72	B	V
[b]12/54	F	79	B	V
[b]53/53	M	68	C	V
637/87	F	78	C	V
484/90	F	69	0	VI
[b]92/73	F	66	C	VI
[b]69/73	F	74	C	VI

[a] Paraffin embedded tissues; [b] PEG embedded tissues; the rest is frozen.

Immunocytochemistry

Immunostaining of free-floating PEG embedded or frozen sections was performed basically using procedures described previously (48) with some modifications. Briefly, incubations were performed with the following primary antibodies for 40–44 h at 4°C. Monoclonal antibody (mAb) AT8 was used at a dilution of 0.1 μg/ml, the polyclonal antibody *GSK-3β Tyrosine-216* to active GSK-3β at 1.5 μg/ml, and the polyclonal antibody *GSK-3β Serine-9* to inactive GSK-3β at 3 μg/ml. Sections were then incubated with biotinylated anti-rabbit IgG or anti-mouse IgM at a dilution of 1:200 for 2 h and were then visualized with the avidin-biotin-peroxidase complex kit (Vector, Burlingame, CA) with 3–3′-diaminobenzidine-4 HCl/H_2O_2 (DAB, Sigma, St. Louis, MO) as substrate. Double immunofluorescent staining was also used, in which CY™3-conjugated anti-rabbit IgG (Jackson ImmunoResearch Laboratories, Inc.,

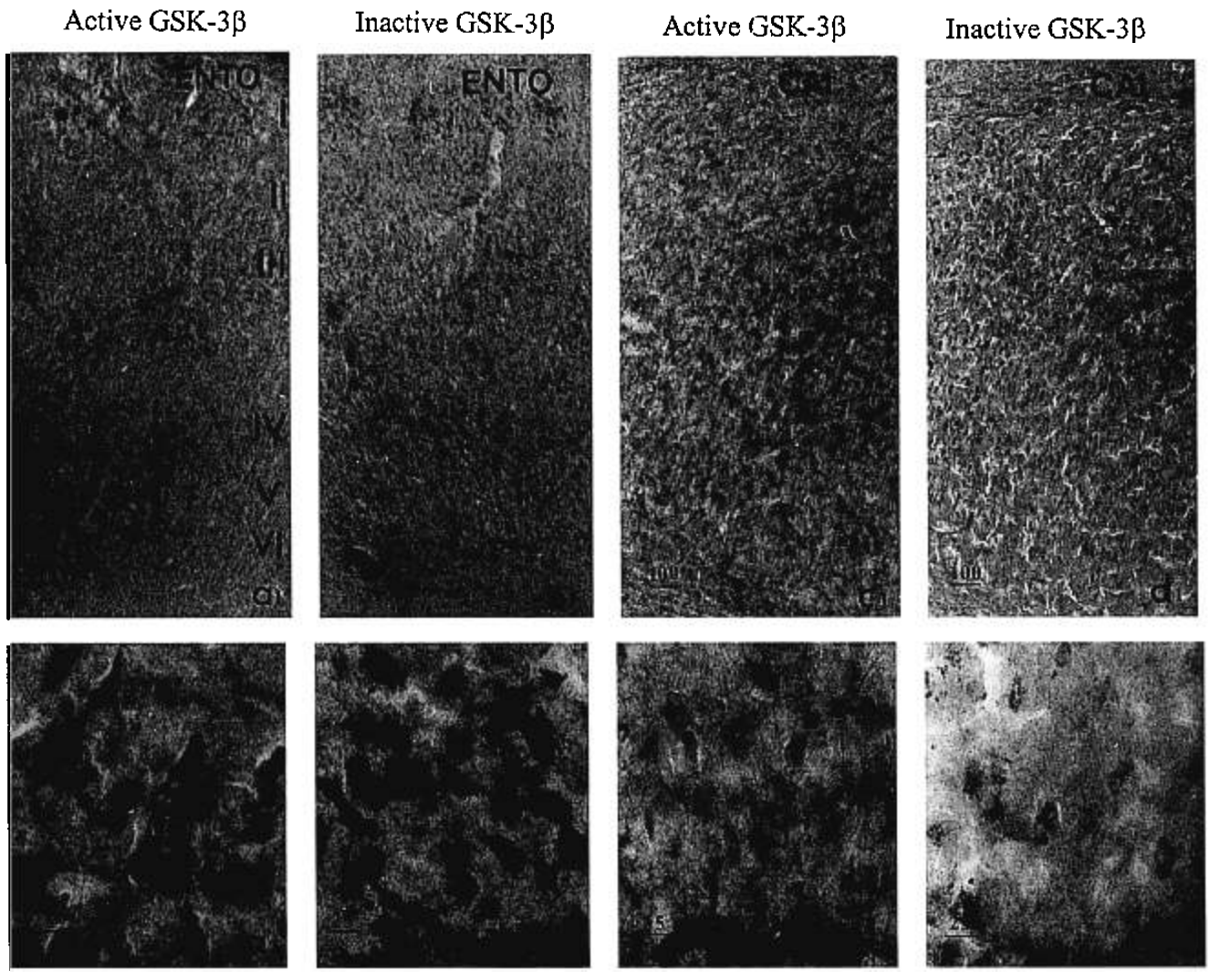

Fig. 1. Immunoreactivity for active (a1, a2, c1, c2) and inactive GSK-3β (b1, b2, d1, d2) in brains at stage 0 neurofibrillary changes. a2 and b2 are the higher magnifications of a1 and b1 Pre-α neurons in entorhinal cortex (ento), respectively. c2 and d2 are the higher magnifications of c1 and d1 pyramidal neurons in CA1, respectively. Layers Pre-α, Pre-β, Pre-γ, Pri-α, Pri-β, and Pri-γ of entorhinal cortex are marked by I, II, III, IV, V, and VI, respectively. Case 1097/96, frozen sections. Magnitudes for scale bars are given in micrometers (μm).

West Grove, PA) was linked to polyclonal antibodies specific to active or inactive form of GSK-3, and CY™2-conjugated anti-mouse IgG (Jackson ImmunoResearch Laboratories, Inc.) linked to mAb AT8.

Immunostaining of paraffin embedded sections was performed following the similar procedures as for free-floating PEG embedded or frozen sections, except that the primary antibody incubations were performed at room temperature overnight. After immunostaining paraffin sections with antibodies to GSK-3β shown by DAB in brown color, sections were subsequently double incubated with mAb AT8 (0.1 or 5 μg/ml), and detected with Vector® SG substrate kit (Vector, Inc.) which yields a blue-grey stain. Some of the paraffin embedded sections were pretreated with 95% formic acid for 2 h before the immunostaining.

The regional and intracellular distributions of AT8 immunoreactivity, active and inactive forms of GSK-3β were based on the immunostainings of frozen, PEG and paraffin embedded sections.

RESULTS

Distribution of Abnormally Hyperphosphorylated Tau, and Active/Inactive GSK-3β Positive Neurons in Brains with Stage 0 Neurofibrillary Changes

AT8 immunoreactivity was not visible in either grey or white matter of the entorhinal, hippocampal and temporal cortices of stage 0 cases. The antibody to active GSK-3β showed moderate staining in cytoplasm in many layer Pre-α neurons and a few neurons in other layers of the entorhinal region, as compared with neighbouring negative neurons (Fig. 1a1, a2). Faint immunoreactivity for active GSK-3β was found in the hippocampal CA1

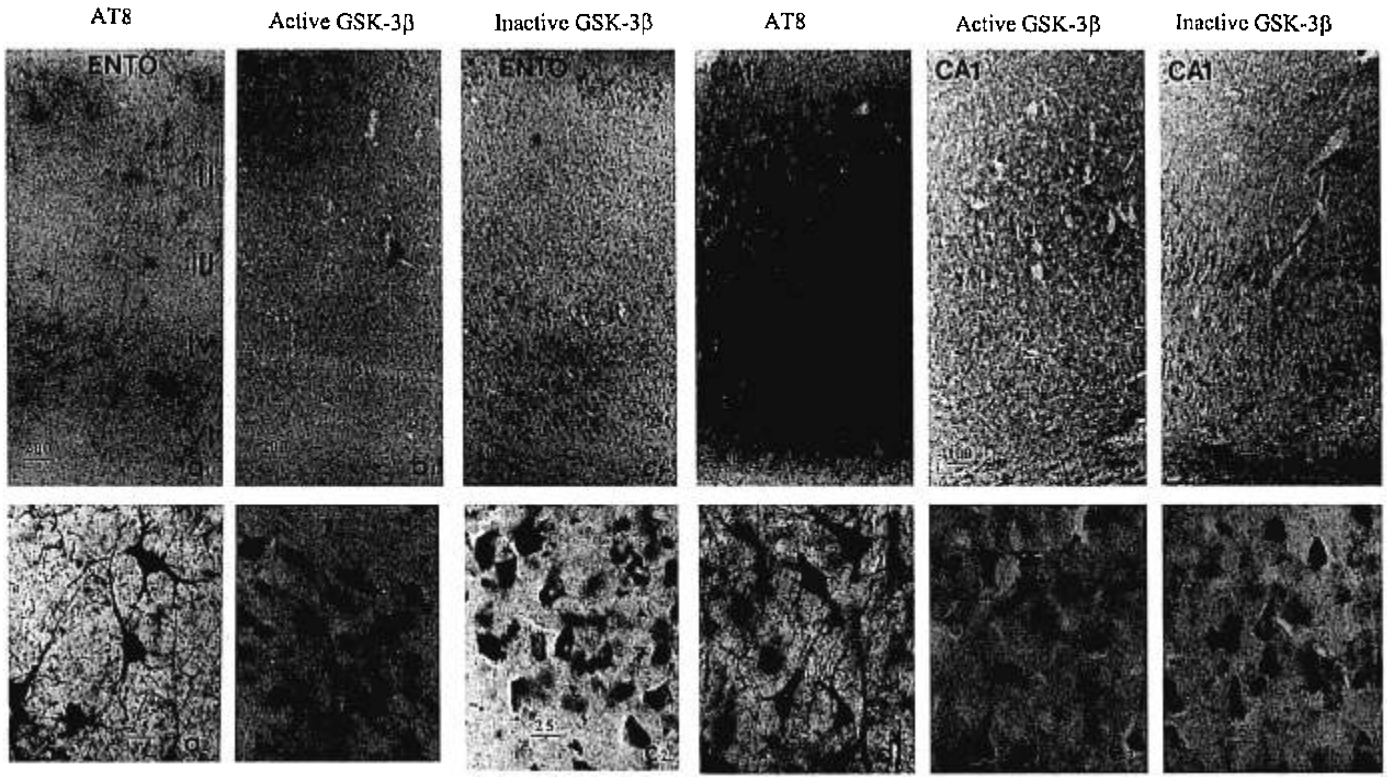

Fig. 2. Immunoreactivity for AT8 (a1, a2, d1, d2), active GSK-3β (b1, b2, e1, e2), and inactive GSK-3β (c1, c2, f1, f2) in brains at stage I/II neurofibrillary change. a2, b2 and c2 are the higher magnifications of a1, b1 and c1 Pre-α neurons in entorhinal cortex (ento), respectively. Layers Pre-α, Pre-β, Pre-γ, Pri-α, Pri-β, and Pri-γ of entorhinal cortex are marked by I, II, III, IV, V, and VI, respectively. d2, e2 and f2 are the higher magnifications of d1, e1 and f1 CA1 pyramidal neurons, respectively. Case 1118/96, frozen sections. Magnitudes for scale bars are given in micrometers (μm).

(Fig. 1c1, c2), and CA2 and temporal cortical pyramidal neurons (not shown).

The antibody to inactive GSK-3β showed more moderately stained neurons in the entorhinal Pre-α layer (Fig. 1b1, b2), as compared with that for active GSK-3β. However, the hippocampal CA2 neurons displayed very intense immunoreactivity for inactive GSK-3β (not shown), whereas the hippocampal CA1 (Fig. 1d1, d2) and temporal cortical pyramidal neurons (not shown) showed moderate immunostaining.

Distribution of Abnormally Hyperphosphorylated Tau, and Active/Inactive GSK-3β Positive Neurons in Brains with Stage I/II Neurofibrillary Changes

Brains at this stage showed some neurons with unchanged morphology and neurons with tangle-like inclusions and NTs positive for AT8 in layers Pre-α and Pri-α of the entorhinal region (Fig. 2a1, a2). Many unchanged neurons and some neurons with tangle-like inclusions positive for AT8 were found in the hippocampal CA1 region (Fig. 2d1, d2). Relatively more unchanged neurons and neurons with tangle-like inclusions positive for AT8 were found in layers Pre-α and Pri-α of the entorhinal cortex and hippocampal CA1 regions of stage II, as compared with stage I (not shown).

A few neurons with tangle-like inclusions positive for active GSK-3β were observed in the Pre-α layer of the entorhinal cortex (Fig. 2b1, b2) but not hippocampal CA1 region (Fig. 2e1, e2) of the brains staged at I/II. Other neurons in the entorhinal cortex and hippocampus were either faintly stained or contained several intensely labelled granules in the cytoplasm. Moderate immunoreactivity for active GSK-3β was seen in neurons of the CA2 region and granule layer of the dentate gyrus, as well as in some neurons in the subiculum (not shown).

In the adjacent sections, immunoreactivity for inactive GSK-3β was strongest in the CA2, CA3 (not shown), and Pre-α layer pyramidal neurons, moderate in the Pre-β, Pre-γ, Pri-α and Pri-γ layers (Fig. 2c1, c2), and CA1 (Fig. 2f1, f2) and CA4 pyramidal neurons, granule cells of the dentate gyrus (not shown), and layers III and V pyramidal neurons of the temporal cortex.

A large number of microglial-like cells positive for active GSK-3β were seen all over the grey and white matter of the entorhinal cortex, hippocampal formation, and temporal cortex of brains staged at 0 and I/II. These cells were more intensely stained than neurons (Figs. 1c2, 2e2). Microglia positive for active GSK-3β appeared to be fewer in number in brains staged at IV, V, and VI, as

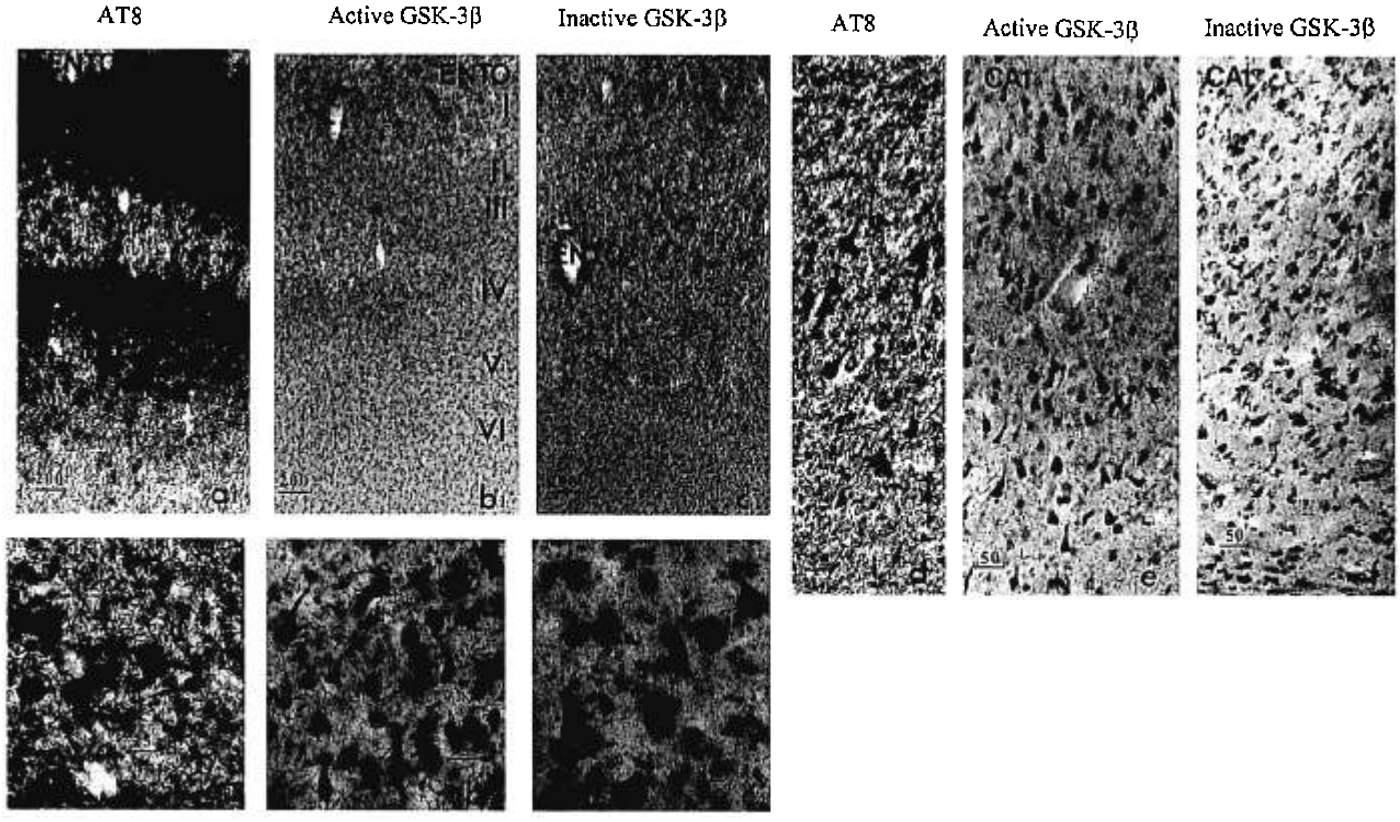

Fig. 3. Immunoreactivity for AT8 (a1, a2, d), active GSK-3β (b1, b2, e), and inactive GSK-3β (c1, c2, f) in staged III/IV brains. a2 is the higher magnifications of a1 lamina dissecans, b2 and c2 are the higher magnifications of b1 and c1 Pre-α neurons, respectively, in entorhinal cortex (ento). Layers Pre-α, Pre-β, Pre-γ, Pri-α, Pri-β, and Pri-γ of entorhinal cortex are marked by I, II, III, IV, V, and VI, respectively. Case 890706, frozen sections. Magnitudes for scale bars are given in micrometers (μm).

compared with the earlier stage brains. This phenomenon was not found for the antibody to inactive GSK-3β.

Distribution of Abnormally Hyperphosphorylated Tau, and Active And Inactive GSK-3β Positive Neurons in Brains with Stage III/IV Neurofibrillary Changes

In comparison with the stage 0 and I/II brains, the stage III/IV brains showed much more severe involvement of neurons with tangle-like inclusions positive for AT8 in the entorhinal (Fig. 3a1, a2), hippocampal CA1 regions (Fig. 3d), and subiculum. Of these, many were late stage tangles (19, 48, 50). The hippocampal CA2, CA3, and CA4 regions, as well as all layers of the temporal cortex, in particular layers III and V, showed AT8 positive tangles and plaques (not shown).

The antibody to active GSK-3β intensely stained neurons with tangle-like inclusions in a similar manner to condensed abnormal tau protein positive for AT8 in all layers of the entorhinal region (Fig. 3b1, b2), and in hippocampal CA1 neurons (Fig. 3e). Many other neurons in these regions showed moderate diffuse staining with this antibody. Some intensely stained tangle-like inclusions were also seen in the subiculum, CA2, CA3, and CA4, as well as in neurons of the granule layer of the dentate gyrus and layers III and V of the temporal cortex. However, the majority of neurons in layers II, III, IV, V, and VI of the temporal cortex were only faintly stained (not shown).

Immunoreactivity for inactive GSK-3β was intense in many neurons of the Pre-α layer and in other layers of entorhinal regions (Fig. 3c1, c2), as well as in the hippocampal CA2, CA3, and CA4 pyramidal neurons (not shown). CA1 pyramidal neurons (Fig. 3f), as well as neurons in the subiculum, granule layer of the dentate gyrus (not shown), and layers II, III and V of the temporal cortex showed moderate staining for inactive GSK-3β. Tangle-like neuronal inclusion was not seen with antibody to inactive GSK-3β.

Distribution of Abnormally Hyperphosphorylated Tau, and Active/Inactive GSK-3β Positive Neurons in Brains with Stage V/VI Neurofibrillary Changes

In stage V/VI brains, AT8 positive tangles were seen throughout the entorhinal cortex (Fig. 4a1, a2), hippocampal regions (Fig. 4d), and temporal cortex (not shown). Tangle-like neuronal inclusions positive for active GSK-3β were also seen throughout the entorhinal

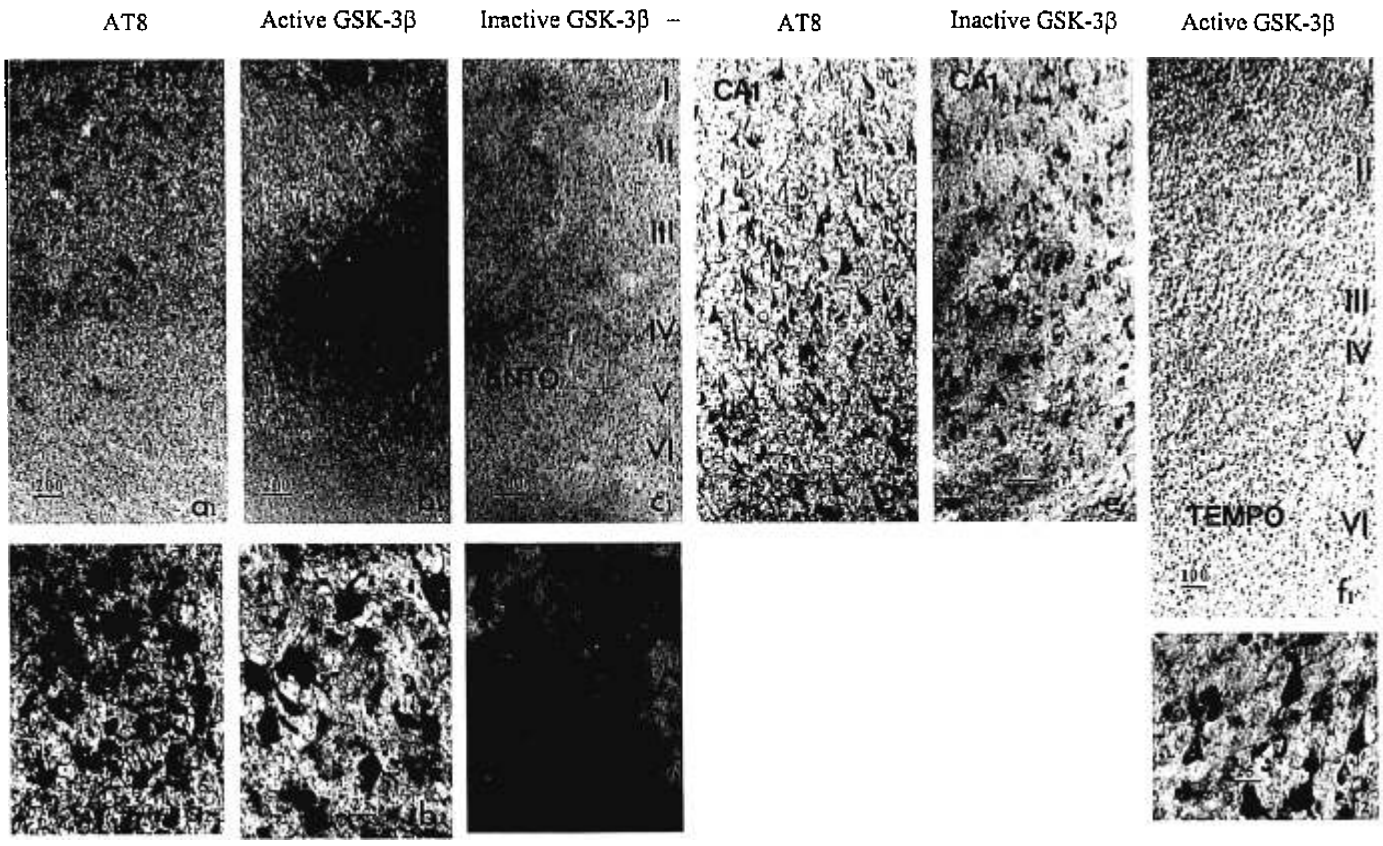

Fig. 4. Immunoreactivity for AT8 (a1, a2, d), active GSK-3β (b1, b2, f1, f2), and inactive GSK-3β (c1, c2, e) in stage V/VI brains. a2, b2 and c2 are the higher magnifications of a1, b1 and c1 Pre-α neurons in entorhinal cortex (ento), respectively. Layers Pre-α, Pre-β, Pre-γ, Pri-α, Pri-β, and Pri-γ of entorhinal cortex are marked by I, II, III, IV, V, and VI, respectively. f2 is the higher magnifications of f1 layer III pyramidal neurons in temporal cortex (tempo). Case 55/53, PEG embedded sections. Magnitudes for scale bars are given in micrometers (μm).

cortex (Fig. 4b1, b2). Many neurons in the temporal cortex, particularly in layers III and V, were intensely stained for active GSK-3β (Fig. 4f1, f2).

The inactive GSK-3β immunoreactivity was moderate in neurons of the entorhinal cortex (Fig. 4c1, c2), subiculum, CA1 (Fig. 4e), CA2, CA3, and CA4 regions (not shown), and in the temporal cortex, especially layers II, III, and V (not shown). None of tangle-like neuronal inclusions were found to be positive for inactive GSK-3β. In addition, similar to those seen in Stages 0/0, I/II and III/IV, some neurons showed intensely stained granules that seem to be associated with lipofuscin pigment.

Patterns of Distribution of Abnormally Hyperphosphorylated Tau, GSK-3β Active/Inactive Forms in Neurons

Immunostaining with mAb AT8 and polyclonal antibody to active GSK-3β permitted classification of 3 patterns of neurons in the entorhinal and hippocampal regions of brains staged at I/II, III/IV, and V/VI.

Pattern 1: Neurons showing accumulation of immunoreactivity for active GSK-3β in intense diffuse granules in the cytoplasm. These neurons have relatively unchanged morphology, but start to accumulate abnormally hyperphosphorylated tau (indicated by small black arrows in Fig. 5A–C, and with bigger white arrow heads in Fig. 6A, B).

Pattern 2: Neurons which showed a mass of active GSK-3β immunoreactivity (indicated by bigger black arrows in Fig. 5A–C) that were proved to tangle by mAb AT8 (not shown) and which showed less than half the cytoplasm occupied by the masses (indicated by bigger black arrows in Fig. 5A–C).

Pattern 3: Neurons which had the mass of active GSK-3β immunoreactivity (indicated by big open arrows in Fig. 5A, B) that were proved to be tangle by mAb AT8 (indicated by small white arrow heads in Fig. 6A, B) and which showed more than half the cytoplasm occupied by tangles (indicated by big open arrows Fig. 5A, B, and by small white arrow heads in Fig. 6A, B).

Some NTs shown by mAb AT8 (Fig. 6A) were found to be positive for active GSK-3β (Fig. 6B). Pattern 1 neurons were seen in paraffin, PEG embedded and frozen sections. Pattern 2 and 3 neurons were only seen in PEG embedded and frozen sections, but not in the paraffin embedded sections, even using pretreatment with 95% formic acid.

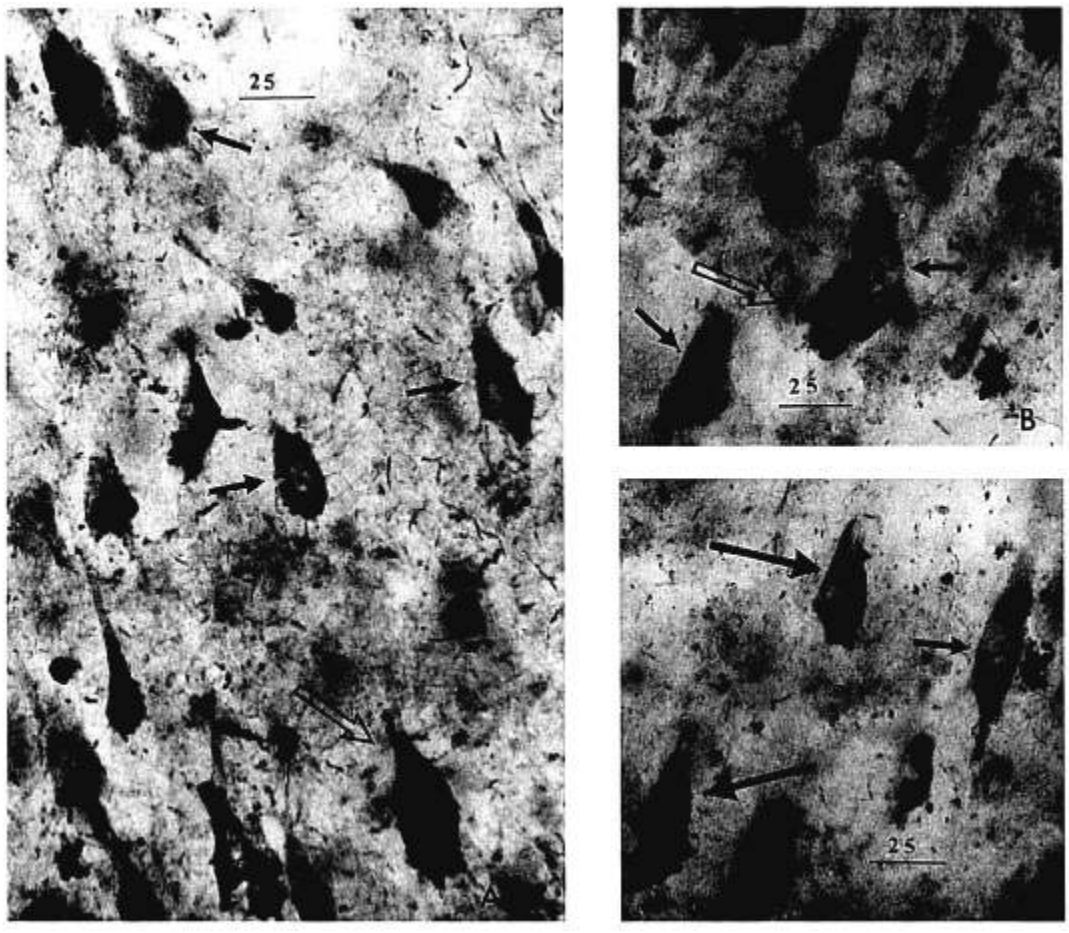

Fig. 5. Active GSK-3β immunoreactivity (A, B and C) in CA1 pyramidal neurons of brains with stage V neurofibrillary changes and stage B amyloid deposition. Pattern 1 indicated by smaller black arrows, Pattern 2 indicated by bigger black arrows and Pattern 3 neurons indicated by open arrows. Case 55/53, PEG embedded sections. Magnitudes for scale bars are given in micrometers (μm).

Some paraffin embedded sections were initially immunostained with the antibody to active GSK-3β, and then double immunostained with mAb AT8. In order to maximally expose any hidden AT8 epitopes, the working concentration of mAb AT8 for double immunostaining was increased from 0.1 μg/ml to 5 μg/ml. Some Pattern 1 neurons remained AT8 negative even when using the higher antibody concentration (not shown).

The antibody to inactive GSK-3β, showed in general moderate cytoplasmic staining of the neurons with unchanged morphology (Figs. 3c2, 4c2). Double immunofluorescent staining using mAb AT8 and antibody to inactive GSK-3β revealed no obvious accumulation of inactive GSK-3β in AT8 positive pretangle neurons and tangle bearing neurons (Fig. 6C, D).

DISCUSSION

To judge a protein kinase as a candidate enzyme involved in PHF-tau formation, 4 general criteria should be taken into consideration. Firstly, the protein kinase should produce a mobility shift of normal tau on electrophoretic gels similar to PHF-tau in vitro. Secondly, up-regulation of protein kinase activity should induce PHF-like tau phosphorylation and impair microtubule assembly and stabilization in intact cells. Thirdly, the protein kinase should be active in neurons, in particular those affected by NFTs. Finally, the protein kinase should occur in all the intracellular and topographic areas where neurofibrillary changes are observed. Previous studies have demonstrated that GSK-3β fulfils the first 2 criteria (14, 15, 18, 29, 30, 36, 39, 44, 45). Due to an inability to detect GSK-3β activity in NFT bearing neurons, no direct in situ evidence supporting GSK-3β as a protein kinase involved in PHF-tau formation has previously been available. Although GSK-3β has been found to be preferentially bound to NFTs (44, 45), the antibodies used in previous studies could not distinguish the active and inactive forms of this enzyme. In order to confirm if GSK-3β is likely to be involved in PHF-tau formation, we used phosphospecific antibodies *GSK-3β Tyrosine-216* and *GSK-3β Serine-9* to compare the distribution of active and inactive forms of GSK-3β, respectively, with that of abnormally hyperphosphorylated tau in the entorhinal

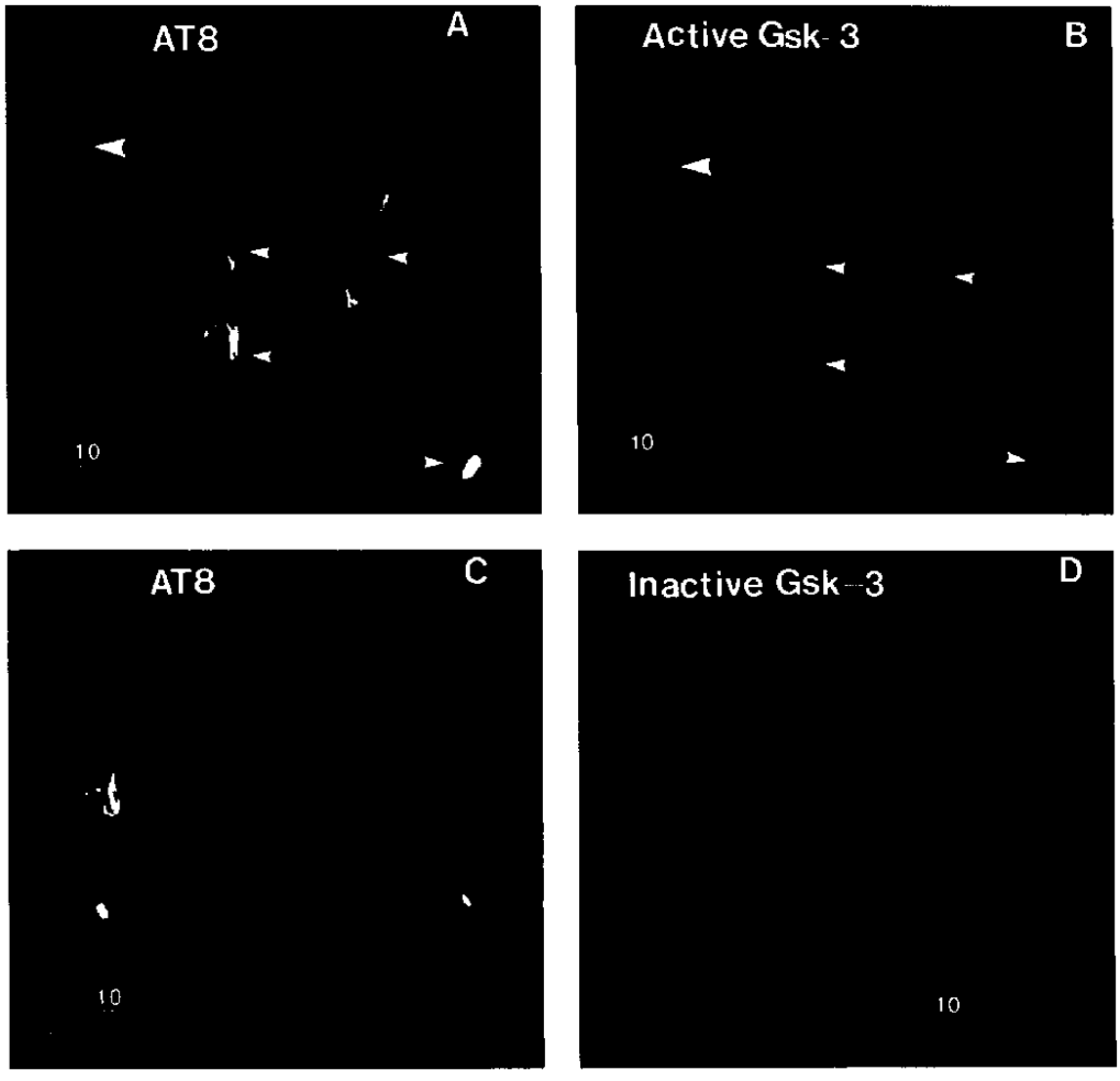

Fig. 6. Double immunofluorescent staining for abnormally hyperphosphorylated tau by mAb AT8 (green, A and C) and polyclonal antibodies to active GSK-3β (red, B) and inactive GSK-3β (red, D) in CA1 pyramidal neurons of brains with stage V neurofibrillary changes and stage B amyloid deposition. Pattern 1 neurons are indicated by bigger white arrow heads and Pattern 3 neurons are indicated by smaller white arrow heads. B and D are from the same field as A and C, respectively. Case 55/53, PEG embedded sections. Magnitudes for scale bars are given in micrometers (μm).

cortex, hippocampal formation, and temporal cortical regions of brains staged for neurofibrillary changes (1). We found that GSK-3β in active form occurs wherever the AD neurofibrillary pathology is observed.

The monoclonal antibody (mAb) AT8 recognizes 6 isoforms of tau in PHF (50). AT8 immunocytochemistry has been used as a complementary method to reveal neurofibrillary changes in brains at different stages (1, 48). Similar to the distribution of neurofibrillary change shown by AT8 immunoreactivity, neurons with accumulation of active GSK-3β positive tangle-like inclusions were initially found in Pre-α and Pri-α layer pyramidal neurons of the entorhinal cortex and hippocampal CA1 pyramidal neurons in brains at the trans-entorhinal (I/II) stages. The involvement of active GSK-3β positive neurons with condensed abnormal tau protein in the entorhinal cortex and hippocampal CA1 region was sequentially more severe when neurofibrillary changes progressed from trans-entorhinal (I/II) to the limbic (III/IV) and eventually isocortical (V/VI) stages (1). Neurons with condensed abnormal tau protein immunopositive for active GSK-3β were also seen in the temporal cortex of brains at isocortical (V/VI) stages, consistent with invasion of neurofibrillary changes to isocortical regions. These data indicate that active GSK-3β is regionally co-distributed with the progressive accumulation of abnormally hyperphosphorylated tau protein.

In addition, we also found that Pattern 1 neurons, which are the pretangle neurons visualized by mAb tau-1 and AT8 (48, 50), appear to accumulate active GSK-3β

in the cytoplasm. Active GSK-3β also appeared to accumulate more in the cytoplasm of Pattern 2 and 3 neurons with condensed abnormal tau protein as NFTs develop. A similar pattern of GSK-3β immunostaining in NFTs has been obtained using R127d, an antibody that does not distinguish the active and inactive forms of this enzyme (45). It is likely that Pattern 1 neurons represent a crucial stage in the formation of abnormally hyperphosphorylated tau in neurons.

Since the accumulated active form of GSK-3β in Pattern 1, 2, and 3 neurons was seen using the antibody against tyrosine-216, it will be important to know what factors maintain the phosphorylation state of this site, in particular whether protein tyrosine phosphatase PTP-1B, whose activity is down-regulated in AD brain, is involved (52). It was previously reported that GSK-3β is inhibited and activated respectively by phosphorylation and dephosphorylation at serine-9 (21). Using the antibody against serine-9, it was found that the inactive form of GSK-3β did not accumulate in Pattern 2 and 3 neurons. Although dephosphorylation of serine-9 by protein phosphatase PP-2A can restore GSK-3β activity in cells (53), this is unlikely in Pattern 2 and 3 neurons, due to an impaired protein phosphatase PP-2A activity (52, 54).

The different intensity of active GSK-3β immunostaining seen in microglial-like cells and neurons of stage 0/0 and I/II brains would imply that GSK-3β activation is cell type specific. The relatively higher levels of active GSK-3β in microglial-like cells of stage 0/0 and I/II brains, as compared with the late neurofibrillary staged brains may provide a reason as to why we were previously unable to show increased levels of GSK-3β activity in AD brains (45). We cannot rule out the possibility that the lower number of active GSK-3β positive microglia in brains at the late stages of neurofibrillary changes is caused by the transformation of activated microglia, making them difficult to distinguish from other structures (55).

In summary, active, but not inactive, GSK-3β is seen to be codistributed with the progressive accumulation of abnormally hyperphosphorylated tau and neurofibrillary changes according to Braak staging. In particular, active GSK-3β accumulation in pretangle neurons supports the idea that GSK-3β is involved in the formation of abnormally hyperphosphorylated tau. The data also suggest that activation of GSK-3β in neurons occurs via phosphorylation at tyrosine-216.

ACKNOWLEDGMENTS

Ute Fertig, Anke Biczysko, and Renate Schneider are thanked for helping with the preparation and immunostaining of sections. Financial support was provided by the Stiftelsen för Gamla Tjänarinnor, Loo and Hans Ostermans Foundation, Sigurd and Elsa Goljes Foundation, the Swedish Medical Research Council, Marianne and Marcus Wallenbergs Foundation, the Deutsche Forschungsgemeinschaft, and NIH grants NS#18105 and AG#08076.

REFERENCES

1. Braak H, Braak E. Neuropathological staging of Alzheimer related changes. Acta Neuropathol 1991;82:239–59
2. Braak H, Braak E, Grundke-Iqbal I, Iqbal K. Occurrence of neuropil threads in the senile human brain and in Alzheimer's disease: A third location of paired helical filaments outside of neurofibrillary tangles and neuritic plaques. Neurosci Lett 1986;65:351–55
3. Grundke-Iqbal I, Iqbal K, Quinlan M, Tung Y-C, Zaide MS, Wisniewski HM. Microtubule-associated protein tau: A component of Alzheimer paired helical filaments. J Biol Chem 1986;261:6084–89
4. Grundke-Iqbal I, Iqbal K, Tung Y-C, Quinlan M, Wisniewski HM, Binder I. Abnormal phosphorylation of the microtubule-associated protein tau in Alzheimer cytoskeletal pathology. Proc Natl Acad Sci USA 1986;83:4913–17
5. Iqbal K, Grundke-Iqbal I, Zaidi T, et al. Defective brain microtubule assembly in Alzheimer disease. Lancet 1986;2:421–26
6. Iqbal K, Grundke-Iqbal I, Smith AJ, George L, Tung Y-C, Zaidi T. Identification and localisation of a tau peptide to paired helical filaments of Alzheimer disease. Proc Natl Acad Sci USA 1989;86: 5646–50
7. Tomlinson BE, Blesses G, Roth M. Observations on the brains of demented old people. J Neurol Sci 1970;11:205–42
8. Alafuzoff I, Iqbal K, Friden H, Adolfsson R, Winblad B. Histopathological criteria for progressive dementia disorders: clinical-pathological correlation and classification by multivariate data analysis. Acta Neuropath 1987;74:209–25
9. Dickson DW, Crystal HA, Mattiace LA, et al. Identification of normal and pathological aging in prospectively studied non-demented elderly humans. Neurobiol Aging 1991;13:179–89
10. Arriagada PV, Growdon JH, Hedley-Whyte ET, Hyman BY. Neurofibrillary tangles but not senile plaques parallel duration and severity of Alzheimer's disease. Neurology 1992;42:631–39
11. Almkvist O, Backman L. Progression in Alzheimer's disease: Sequencing of neuropsychological decline. Int J Geriatr Psychiatry 1993;8:755–63
12. Braak H, Duyckaerts C, Braak E, Piette F. Neuropathological staging of Alzheimer-related changes correlates with psychometrically assessed intellectual status. In: Corian B, Iqbal K, Nicolini M, Winblad B, Wisniewski H, Zatta P, eds. Alzheimer's disease: Advances in clinical and basic research. Third International Conference on Alzheimer's Disease and Related Disorders. Chichester: John Wiley & Sons, 1993:131–37
13. Geula C, Mesulam M-M, Saroff DM, Wu C-K. Relationship between plaques, tangles, and loss of cortical cholinergic fibers in Alzheimer disease. J Neuropathol Exp Neurol 1998;57:63–75
14. Ishiguro K, Takamatsu M, Tomizawa K, et al. Tau protein kinase I converts normal tau protein into A68 like component of paired helical filaments. J Biol Chem 1992;267:10897–901
15. Mandelkow E-M, Drewes G, Biernat J, et al. Glycogen synthase kinase-3 and the Alzheimer-like state of microtubule-associate protein tau. FEBS Lett 1992;314:315–21
16. Drewes G, Lichtenberg-Kraag B, Doering F. Mitogen-activated protein (MAP) kinase transforms tau protein into an Alzheimer-like state. EMBO J 1992;6:2132–38
17. Ledesma MD, Correas I, Avila J, Diaz-Nido J. Implication of brain cdc2 and MAP2 kinases in the phosphorylation of tau protein in Alzheimer's disease. FEBS Lett 1992;308:218–24
18. Sengupta A, Wu Q, Grundke-Iqbal I, Iqbak K, Singh TJ. Potentiation of GSK-3-catalysed Alzheimer-like phosphorylation of human tau by cdk5. Mol Cell Biochem 1997;167:99–105
19. Pei J-J, Grundke-Iqbal I, Iqbal K, Bogdanovic N, Winblad B, Cowburn RF. Accumulation of cyclin-dependent kinase 5 (cdk5) in neurons with early stages of Alzheimer's disease neurofibrillary degeneration. Brain Res 1998;797:267–77

20. Cohen P, Yellowlees D, Aitken A, Donella-Deana A, Hemmings BA, Parker PJ. Separation and characterization of glycogen synthase kinase-3, glycogen synthase kinase-4 and glycogen synthase kinase-5 from rabbit skeletal muscle. Eur J Biochem 1982;124:21–35
21. Cohen P, Alessi DR, Cross DAE. PDK1. One of the missing links in insulin signal transduction? FEBS Lett 1997;410:3–10
22. Stambolic V, Woodgett JR. Mitogen inactivation of glycogen synthase kinase-3 β in intact cells via serine 9 phosphorylation. Biochem J 1994;303:701–4
23. Cross DA, Alessi DR, Cohen P, Andjelkovich M, Hemmings B. Inhibition of glycogen synthase kinase-3 by insulin mediated by protein kinase B. Nature 1995;378:785–89
24. Eldar-Finkelman H, Seger R, Vandenheede JR, Krebs EE. Inactivation of glycogen synthase kinase-3 by epidermal growth factor is mediated by mitogen-activated protein kinase/p90 ribosomal protein S6 kinase signaling pathway in NIH/3T3 cells. J Biol Chem 1995;270:987–90
25. Hughes K, Nikolakaki E, Plyte SE, Totty NF, Woodgett JR. Modulation of glycogen synthase kinase-3 family by tyrosine phosphorylation. EMBO J 1993;12:803–8
26. Cross DA, Alessi DR, Vandenheede JR, McDowell HE, Hundal HS, Cohen P. The inhibition of glycogen synthase kinase-3 by insulin or insulin-like growth factor 1 in the rat skeletal muscle cell line L6 is blocked by wortmannin, but not by rapamycin: Evidence that wortmannin blocks activation of the mitogen-activated protein kinase pathway in L6 cells between Ras and Raf. Biochem J 1994;303:21–26
27. Murai H, Okazaki M, Kikuchi A. Tyrosine dephosphorylation of glycogen kinase-3 is involved in its extracellular signal-dependent inactivation. FEBS Lett 1996;392:153–60
28. Ishiguro K, Shiratsuchi A, Sato S, et al. Glycogen synthase kinase 3β is identical to tau protein kinase I generating several epitopes of paired helical filaments. FEBS Lett 1993;325:167–72
29. Mulot SF, Hughes K, Woodgett JR, Anderton BH, Hanger DP. PHF-tau from Alzheimer's brain comprises four species on SDS-PAGE which can be mimicked by in vitro phosphorylation of human brain tau by glycogen synthase kinase-3 beta. FEBS Lett 1994;349:359–64
30. Imahori K, Uchida T. Physiology and pathology of tau protein kinases in relation to Alzheimer's Disease. J Biochem 1997;121:179–88
31. Hanger DP, Hughes K, Woodgett JR, Brion JP. Glycogen synthase kinase-3 induces Alzheimer's disease-like phosphorylation of tau: Generation of paired filament epitopes and neuronal localisation of the kinase. Neurosci Lett 1992;147:58–62
32. Yang S-D, Jau-Song Y, Shine-Gwo S, Jun-Jae H. Protein kinase Fa/Glycogen synthase kinase-3α after heparin potentiation phosphorylates tau on sites abnormally phosphorylated in Alzheimer's disease brain. J Neurochem 1994;63:1416–25
33. Song J-S, Yang S-D. Tau protein kinase I/GSK-3 beta/kinase FA in heparin phosphorylates tau on Ser199, Thr231, Ser235, Ser262, Ser369, and Ser400 sites phosphorylated in Alzheimer disease brain. J Prot Chem 1995;14:95–105
34. Shiurba RA, Ishiguro K, Takashi M, et al. Immunocytochemistry of tau phosphoserine 413 and tau protein kinase I in Alzheimer pathology. Brain Res 1996;737:119–32
35. Singh TJ, Grundke-Iqbal I, Iqbal K. Differential phosphorylation of human tau isoforms containing three repeats by several protein kinase. Arch Biochem Biophys 1996;328:43–50
36. Lovestone S, Hugh-Reynolds C, Latimer D, et al. Alzheimer's disease-like phosphorylation of the microtubule-associated protein tau by glycogen synthase kinase-3 in transfected mammalian cells. Current Biology 1994;4:1077–86
37. Sperber BR, Leight S, Goedert M, Lee VM-Y. Glycogen synthase kinase-3β phosphorylates tau protein at multiple sites in intact cells. Neurosci Lett 1995;197:149–53
38. Wagner U, Utton M, Gallo J-M, Miller CCJ. Cellular phosphorylation of tau by GSK-3β influences tau binding to microtubules and microtubule organization. J Cell Sci 1996;109:1537–43
39. Utton MA, Vandecandelaere A, Wagner U, et al. Phosphorylation of tau by glycogen synthase kinase 3-beta affects the ability of tau to promote microtubule self-assembly. Biochem J 1997;323:741–47
40. Hong M, Chen DCR, Klein PS, Lee VM-Y. Lithium reduces tau phosphorylation by inhibition of glycogen synthase kinase-3. J Biol Chem 1997;272:25332–62
41. Hong M, Lee VM-Y. Insulin and insulin-like growth factor-1 regulate tau phosphorylation in cultured human neurons. J Biol Chem 1997;272:19547–53
42. Woodgett JR. Molecular cloning and expression of glycogen synthase kinase-3/Factor A. EMBO J 19990;9:2431–38
43. Takahashi M, Tomizawa K, Ishiguro K, Takamatsu M, Fujita SC, Imahori K. Involvement of τ protein kinase I in paired helical filament-like phosphorylation of the juvenile τ in rat brain. J Neurochem 1995;64:1759–68
44. Yamaguchi H, Ishiguro K, Uchida T, Takashima A, Lemere CA, Imahori K. Preferential labeling of Alzheimer neurofibrillary tangles with antisera for tau protein kinase (TPKI)/glycogen synthase kinase-3β and cyclin-dependent kinase 5, a component of TPK II. Acta Neuropathol 1996;92:232–41
45. Pei J-J, Tanaka T, Tung Y-C, Braak E, Iqbal K, Grundke-Iqbal I. Distribution, levels and activity of glycogen synthase kinase-3 in the Alzheimer disease brain. J Neuropath Exp Neurol 1997;6:70–78
46. Braak H, Braak E, Ohm T, Bohl J. Silver impregnation of Alzheimer's neurofibrillary changes counterstained for basophilic material and lipofuscin pigment. Stain Technol 1988;63:197–200
47. Gallyas F. Silver staining of Alzheimer's neurofibrillary changes by means of physical development. Acta Morphol Acad Sci Hung 1971;19:1–8
48. Braak E, Braak H, Mandelkow E-M. A sequence of cytoskeleton changes related to the formation of neurofibrillary tangles and neuropil threads. Acta Neuropath 1994;87:554–67
49. Campbell SK, Switzer RC, Martin TL. Alzheimer's plaques and tangles: A controlled and enhanced silver-staining method. Soc Neurosci Abstr 1987;13:678
50. Bancher C, Brunner C, Lassmann H, et al. Accumulation of abnormally phosphorylated tau precedes the formation of neurofibrillary tangles in Alzheimer's disease. Brain Res 1989;477:90–99
51. Wischik CM, Lai R, Edwards PC, et al. Quantitative analysis of tau protein in paired helical filament (PHF) preparations: Implications for the role of tau phosphorylation in PHF assembly in Alzheimer's disease. Neurobi Aging 1995;16:409–17
52. Gong C-X, Singh TJ, Grundke-Iqbal I, Iqbal K. Phosphoprotein phosphatase activities in Alzheimer disease. J Neurochem 1993;61:921–27
53. Shaw M, Cohen P, Alessi DR. Further evidence that the inhibition of glycogen synthase kinase-3β by IGF-1 is mediated by PDK1/PKB-induced phosphorylation of Ser-9 and not by dephosphorylation of Tyr-216. FEBS Lett 1997;416:307–11
54. Gong C-X, Shaikh S, Wang J-Z, Zaidi T, Grundke-Iqbal I, Iqbal K. Phosphatase activity toward abnormally phosphorylated τ: Decrease in Alzheimer disease brain. J Neurochem 1995;65:732–38
55. Kreutzberg GW. Microglia: A sensor for pathological events in the CNS. TINS 1996;19:312–18

Received January 19, 1999
Revision received May 7, 1999
Accepted May 10, 1999